Ionics (2011) 17:535–543
DOI 10.1007/s11581-011-0552-4

ORIGINAL PAPER

Effect of biotite content of hydrogels on enhanced removal of methylene blue from aqueous solution

Yi Liu · Yian Zheng · Aiqin Wang

Received: 16 January 2011 / Revised: 21 February 2011 / Accepted: 28 March 2011 / Published online: 20 April 2011

Abstract A series of chitosan-*g*-poly(acrylic acid)/biotite (CTS-*g*-PAA/BT) hydrogels with unique clay biotite (BT) were prepared and used to remove cationic dye methylene blue (MB) from aqueous solution by batch adsorption experiments. Variables of the system including BT content, initial pH, contact time, initial concentration, and temperature affecting the adsorption efficiency of MB by CTS-*g*-PAA/BT hydrogels were investigated. Kinetic studies indicated that the adsorption data well followed pseudo-second-order kinetics. Langmuir and Freundlich isotherm models were applied to experimental equilibrium data of MB adsorption depending on temperature. The adsorption equilibrium data obeyed Langmuir isotherm, and the monolayer adsorption capacity calculated from the Langmuir isotherm was 2,125.70 mg/g for CTS-*g*-PAA/10% BT at 30 °C. The adsorption capacity was much higher compared with other hydrogels with the same content of other clays. The introduction of BT into the hydrogel could effectively improve its adsorption properties and reduce the cost. Thermodynamic parameters were evaluated for the dye-adsorbent systems and revealed that the adsorption process was spontaneous and exothermic in nature. All the information gave an indication that CTS-*g*-PAA/10% BT could potentially be applied as an efficient adsorbent for cationic dye removal from aqueous solution.

Keywords Hydrogel · Biotite · Methylene blue · Adsorption equilibrium · Kinetics

Y. Liu · Y. Zheng · A. Wang (✉)
Center of Eco-material and Green Chemistry, Lanzhou Institute of Chemical Physics, Chinese Academy of Sciences,
Lanzhou 730000, People's Republic of China
e-mail: aqwang@licp.cas.cn

Y. Liu · Y. Zheng
Graduate University of the Chinese Academy of Sciences,
Beijing 100049, People's Republic of China

Introduction

Being highly colored, dyes are readily apparent in wastewater even in very low concentration. Thus, the presence of dyes in the water resources is undesirable. In addition, the colored wastewater in the receiving streams can reduce the light penetration, thus limiting the depuration by natural oxidation. Consequently, the presence of toxic dyes in aqueous streams poses a direct threat to environment and human and has gained worldwide attention. Many techniques such as ion exchange [1], chemical precipitation [2], coagulation [1], ozonation [3], and adsorption [4] have been developed to remove these toxic dyes from aqueous solution. Among these techniques, adsorption is considered as a preferred and effective technique due to that it can deal with various concentrations of dyes and it does not induce the formation of hazardous materials. The most widely employed adsorbent is activated carbon due to its pore structure, high efficiency, and adsorption capacity for some dyes, but the cost and difficulty in separation after adsorption hinder its large-scale application [5]. Several low-cost adsorbents such as vermiculite [6], hazelnut shell [7], and rice husk ash [8] have also been investigated for decontamination purpose; however, the adsorption capacities of these adsorbents were restricted. Therefore, many researchers have taken up with seeking for more effective adsorbents to eliminate these hazardous dyes from the effluent from the viewpoints of environment and scientific and technological importance.

Recently, hydrogels have attracted extensive attention for dye removal because of their excellent characteristics such as high molecular and oxygen permeability and low interfacial tension [9]. Hydrogels are three-dimensional polymeric network with variety of functional groups such as hydroxyl, amine, carboxylic acid, and sulfonic acid groups which can adsorb or trap ionic dyes, such as methylene blue (MB) from aqueous solution [10]. Bekiari

and coworkers prepared poly(*N, N*-dimethylacrylamide-*co*-sodium acrylate) hydrogel and found that the hydrogel had strong affinity for cationic dyes and weak affinity for hydrophobic dyes [11]. Taking into account of the limitation of the pure polymeric hydrogels, like poor gel strength and stability, some inorganic clay materials including mica, montmorillonite, vermiculite, and sepiolite have been incorporated into pristine hydrogels for the synthesis of organic–inorganic hybrid hydrogels [12–15]. Clays have high mechanical strength and chemical stability, and are natural, plentiful, and cheap materials. As a consequence, the preparation of organic–inorganic hydrogel has received increasing attention. Zheng and coworker prepared chitosan-*g*-poly(acrylic acid)/rectorite composites and used them as the adsorbents to treat wastewater, with the discovery that these hydrogels exhibited a potential application for the fast removal of ammonium nitrogen from aqueous solution and could be applied to various adsorption systems [16]. Recently, Wang and coworkers gained chitosan-*g*-poly(acrylic acid)/attapulgite composite and found that the composites could remove MB quickly from aqueous solution [17].

Biotite (BT) is a 2:1 phyllosilicate material, in possession of ample hydroxyl groups on its surface, which can copolymerize with hydrophilic vinyl monomers, and then is expected to prepare organic–inorganic hydrogel. The unique structure of BT is that the 2:1 layer with octahedrally coordinated cations sandwiched between two sheets of Si, Al tetrahedral, and the main cations in the octahedral layer are Mg and Fe (II); the latter ion can control the redox state of associated solutes. Based on these considerations, a series of chitosan-*g*-poly(acrylic acid)/biotite (CTS-*g*-PAA/BT) hydrogels were synthesized in this study and employed to remove cationic dye MB from aqueous solution. The experiments were performed systematically to investigate the effects of several experimental parameters including BT content, pH of dye solution, contact time, initial dye concentration, and temperature on the adsorption capacities. In addition, adsorption isotherms, and kinetics for the adsorption of MB onto the hydrogels were also investigated. Finally, the adsorption mechanism was also proposed.

Experimental

Materials

Acrylic acid (AA, chemically pure, distilled before use), ammonium persulfate (APS, analytical grade, recrystallized from distilled water before use) and *N, N*'-methylenebisacrylamide (MBA, chemically pure, used as received) were purchased from Shanghai Reagent Corp. (Shanghai, China). Chitosan (CTS) with deacetylation degree of 0.90 and viscosity-average molecular weight of 3.0×10^5 g/mol was obtained from Zhejiang Yuhuan Ocean Biology Co. (Zhejiang, China). Biotite (BT, Shijiazhuang Chenxing Industry Co. Ltd., Hebei, China) was milled through a 320-mesh screen before use. Methylene blue (MB) was purchased from Alfa Aesar A Johnson Matthey Company and used without further purification. Other reagents used were all of analytical grade, and all solutions were prepared with distilled water.

The preparation of CTS-g-PAA/BT hydrogels

CTS-*g*-PAA/BT was prepared similar to our previous report [16]. Typically, 0.5 g CTS was dissolved in 30 ml acetic acid solution (1%) in a 250-ml four-neck flask equipped with a mechanical stirrer, a reflux condenser, a funnel, and a nitrogen line. APS (0.10 g) was added into the flask to initiate CTS to produce radicals after being purged with nitrogen for 30 min to remove oxygen dissolved in the system. Ten minutes later, the mixture of 3.60 g AA, 0.15 g MBA, different amounts of BT, and 10 ml distilled water was added. The water bath was kept at 70 °C for 3 h to accomplish the reaction, and the resulting granular product was washed with distilled water to remove remanent reactants and then transferred into 1 mol/L NaOH solution to be neutralized to pH=7. Thereafter, the swollen sample was dehydrated with industrial ethanol and dried to a constant weight at 70 °C. The sample was milled through a 200-mesh screen and employed for subsequent experiments. CTS-*g*-PAA hydrogel was prepared in the light of a similar procedure except without BT.

Adsorption studies

Adsorption tests were conducted on thermostated shaker (THZ-98A) at a constant speed of 120 rpm in a 100-mL conical flask with a stopper. To study the effect of important parameters such as content of BT, pH of MB solution, contact time, initial MB concentration, and temperature on MB removal, batch experiments were carried out with 50 mL MB solution of known concentration and 0.025 g adsorbent in systems. Effect of content of BT was investigated with a series of adsorbents and MB solution (pH=7) mixture in each flask for 240 min to determine the optimum adsorbents for further adsorption experiments. Effect of pH on MB removal was studied over a pH range 2~9, and solution pH was adjusted by the addition of 0.1 mol/L NaOH or HCl solutions using a pHS-25 pH-meter. Effect of contact time on MB removal was done at pH 7 with initial MB concentration of 1,000 mg/L at predetermined time intervals. For isotherm studies, a

series of flasks with MB solution in the range of 950~1,200 mg/L at pH 7 were prepared, and then, the adsorbent was added to each flask. The mixtures were agitated at constant temperatures of 30, 40, and 50 °C for 240 min. The suspension was centrifuged at 5,000 rpm for 10 min. The residual MB concentration in the adsorption media was determined at the maximum adsorption wavelength of 670 nm using a Specord 200UV/vis spectrophotometer. Calibration curve was plotted between absorbency and MB concentration.

The adsorption capacity was calculated by the equation as follows:

$$q = (C_i - C_f) \times V/W \quad (1)$$

where q (mg/g) represents MB removal by the adsorbent; C_i and C_f (mg/L) represent MB concentration before and after adsorption, respectively; V (L) is MB solution volume used; and W (g) is the weight of adsorbent.

Desorption experiment

The desorption of MB loaded on as-prepared hydrogels was carried out with distilled water and 0.1 M hydrochloric acid as desorbing agents. MB loaded adsorbents (0.050 g) were contacted separately with 50 mL desorbing agent solutions and kept stirring at 30 °C, 120 rpm for 90 min. Then, the desorbed amount of MB was obtained.

Characterization

Infrared spectra of the samples were recorded on a Thermo Nicolet, NEXUS, TM Spectrophotometer (Madison, USA) in the range of 4,000~400 cm^{-1} using KBr pellet. The spectrum was collected 32 times and corrected for the background noise.

Results and discussion

FTIR spectra of adsorbents

FTIR spectra of BT, CTS-*g*-PAA, and CTS-*g*-PAA/BT with 10 wt% BT (CTS-*g*-PAA/10% BT) were shown in Fig. 1. A broad band at about 3,600~3,300 cm^{-1} and the band at 1,629 cm^{-1} were ascribed to the stretching and bending vibrations of −OH of water molecules in the interlayer of BT, respectively. The bands at 1,728, 1,555, and 1,463 cm^{-1}, corresponding to −COOH stretching, C=O asymmetric stretching, and C=O symmetric stretching, respectively, and the band at 1,325 cm^{-1} corresponding to C–N stretching were shifted and reduced in the spectrum of CTS-*g*-PAA/10% BT. In addition, the band at 999 cm^{-1} corresponding to stretching vibration of Si-O bond had shifted and almost disappeared in the spectrum of CTS-*g*-PAA/10% BT, while a new absorption band at 1,033 cm^{-1} corresponding to stretching vibration of Si–O–Si bond appeared, suggesting the reaction between the $-COO^-$ and −OH on the surface of BT micropowder.

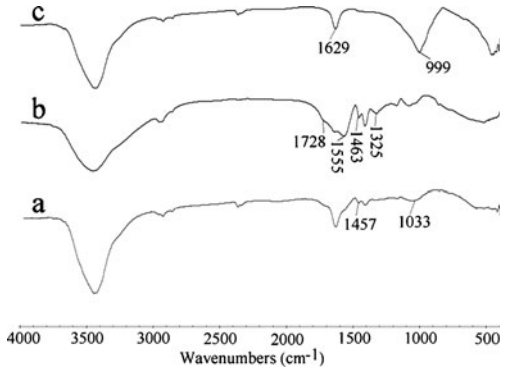

Fig. 1 The spectra of CTS-*g*-PAA/10% BT (*a*), CTS-*g*-PAA (*b*), and BT (*c*)

Effect of BT content

The introduction of clay component into a hydrogel thus resulting in interactions between organic composite and clay may have effects on the properties of both clay and organic composite [18]. In this section, the effect of BT content on adsorption capacity toward MB was investigated, as shown in Table 1. As can be seen, the adsorption capacity reduced as increasing BT, but the adsorption efficiency of CTS-*g*-PAA/10% BT was comparable to that of CTS-*g*-PAA. Furthermore, the adsorption capacity of CTS-*g*-PAA/10% BT toward MB was higher than those of other hydrogels with 10 wt% of corresponding clays (Table 2). This meant the particularity and value of the introduction of BT into the hydrogel. The results presumably attributed to that when the BT content was low (10 wt%), the BT was facilely ionized and distributed into CTS-*g*-PAA hydrogel, which correspondingly enhanced MB removal to a certain extent [19]. An appropriate addition of BT can improve the polymeric network, which was convenient for the penetration of MB into the polymeric network, and thus enhanced the adsorption capacity. When the BT content was high (above 10 wt%), more BT particles served as additional network point to facilitate the reaction between more −OH and $-COO^-$ in the hydrogel, reducing thus activated points and decreasing the elasticity of the hydrogel, and accordingly, the adsorption capacity toward MB was reduced [12, 20]. Based on the above analysis, the adsorption characteristics of CTS-*g*-PAA and CTS-*g*-PAA/10% BT were studied in detail for the further experiments.

Table 1 Relationship between the BT content and adsorption capacity toward MB

BT content (wt%)	0	10	30	100
Adsorption capacity (mg/g)	2,010.73	2,002.49	1,309.43	8.98

Effect of pH

The pH of dyes solution is one of the major factors influencing dye removal, especially for ionic dyes [21]. The molecular structure and forms of functional groups on the surface of an adsorbent may vary according to different pH of dye solution [22]. The hydrogen and hydroxyl ions are adsorbed quite strongly, and thus, the adsorption of the other ions is affected by the pH of the solution. Different materials adsorb onto diverse adsorbents may bring into divergent ranges of suitable pH region for adsorption. Therefore, it was essential to study the effect of pH on adsorption, and the variation of MB adsorption on both adsorbents over a broad range of pH (2~9) was shown in Fig. 2. It was obvious that the adsorption capacity increased as increasing pH for the both adsorbents, and significant enhancement reached for MB adsorption before pH 4, but when pH value attained 5, the adsorption capacities increased hardly. The adsorption of charged dye onto an adsorbent surface is greatly influenced by the charge on the surface of the adsorbent which in turn is influenced by pH of the dye solution. It is known that only a small amount of CTS was used in the preparation of the hydrogels and most of the active amine groups on the CTS have taken part in the copolymerization process, so carboxyl groups within the polymeric networks played important role in controlling the adsorption properties of the hydrogels. Accordingly, the possible reason is as follows: at lower pH, most of the carboxyl groups on the surface of the adsorbent exist in the form of −COOH, and meantime the competition between hydrogen ion and cationic dye MB increasing, then reducing MB removal. At higher pH, more carboxyl groups occur in the form of $-COO^-$, thus increasing the electrostatic force between adsorbent and MB, therefore enhancing adsorption toward MB. As reported, the p*K*a of poly (acrylic acid) is about 4.7 [23], and then, the group −COOH can be facilely ionized above pH value of 4.7. As pH attained 5, the adsorption capacities increased hardly owing to the buffer action of −COOH and $-COO^-$ groups.

Effect of contact time

The adsorption uptake versus contact time was investigated to find out the equilibrium time for maximum adsorption, as illustrated in Fig. 3. It was clear that the adsorption capacity increased promptly in the first time slot (0~60 min), but after the contact time reached 60 min, the adsorption capacity almost remained unchanged. Thereby, the equilibrium time of the studied experimental system was 60 min. In addition, the time-rate curves are single, continuous, and leading to saturation, indicating the possible monolayer coverage of MB onto the both adsorbents surfaces [24].

Adsorption kinetics

The adsorption data were analyzed in terms of pseudo-first-order and pseudo-second-order kinetic models to understand adsorption mechanism. Lagergren's pseudo-first-order [25] and Ho's pseudo-second-order models [26] are two important models applied for solid–liquid adsorption systems. The two models were described by the following expressions, respectively:

$$\log(q_{1e} - q_t) = \log q_{1e} - k_1 t/2.303 \quad (2)$$

$$t/q_t = 1/\left(k_2 q_{2e}^2\right) + t/q_{2e} \quad (3)$$

where q_{1e}, q_{2e}, and q_t represent the amount of dye adsorbed per unit mass of adsorbent at equilibrium and at any time t, respectively. The parameters k_1 (min^{-1}) and k_2 (g/(mg min)) are the rate constants of the pseudo-first-order and pseudo-second-order models, respectively. The slope and intercept of the plot log (q_{1e}–q_t) against t can be obtained k_1 and q_{1e}, and as such, q_{2e} and k_2 can be obtained from the plot t/q_t versus t.

Based on the parameters in Table 3, the R^2 values of pseudo-second-order model were found to be higher than those of pseudo-first-order model, which indicated that the experimental data were fitted to pseudo-second-order kinetic model for MB onto both adsorbents. In addition, the calculated q_{2e} values from pseudo-second-order model were close to those of experimental q_{exp}, validating the results mentioned above.

Table 2 The adsorption capacities of several hydrogels with 10 wt% clays toward MB

Adsorbent	Adsorption capacity (mg/g)	Reference
CTS-*g*-PAA/10% MMT	<1,875	[13]
CTS-*g*-PAA/10% VMT	1,612.32	[14]
CTS-*g*-PAA/10% APT	1,870	[17]
CTS-*g*-PAA/10% BT	2,002.49	This paper

CTS-g-PAA chitosan-*g*-poly(acrylic acid), *MMT* montmorillonite, *VMT* vermiculite, *APT* attapulgite

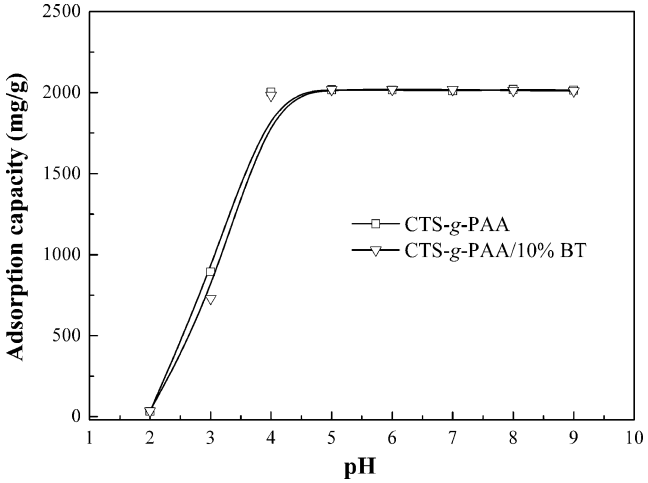

Fig. 2 Effect of pH on adsorption

Effect of initial concentration and solution temperature

Figure 4 showed the amount adsorbed as a function of initial concentration at different temperatures. Apparently, initial concentration played an important role in affecting the amount adsorbed. As can be seen, MB uptake increased as increasing initial concentration, and reached a plateau when the initial concentration was 1,150 mg/L for both adsorbents in the range of the temperature studied. The initial MB concentration affords the essential driving force to overcome the resistances to the mass transfer of MB between the aqueous and solid phases [27]. The higher the initial MB concentration, the stronger the driving force of concentration gradient, and thus the higher adsorption capacity. But as the initial concentration was higher than 1,150 mg/L, the adsorption sites of both the adsorbent were completely occupied, thus making the adsorption capacity constant. It can be seen that temperature also affected MB removal and low temperature was favorable for the studied adsorption system. Furthermore, it was obvious that MB uptake decreased with further increase in temperature, meaning that the MB adsorption process was exothermic. The results probably attributed to that equilibrium adsorption capacity of an adsorbent for a particular adsorbate may change as changing temperature [28].

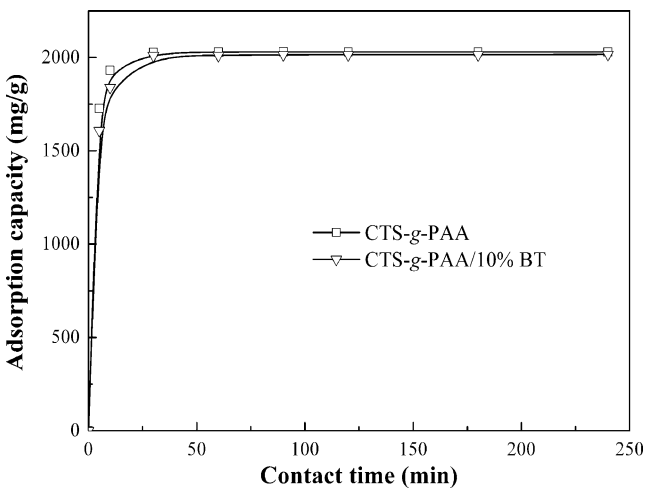

Fig. 3 Effect of contact time on adsorption

Adsorption isotherms

The adsorption isotherm suggests how an adsorbate distributes between the liquid phase and the solid phase when the adsorption process reaches an equilibrium state, and analysis of the equilibrium data is essential to optimize the adsorption system. Certain constants of an adsorption isotherm express the surface properties and affinity of the adsorbent. The adsorption equilibrium data were analyzed by Langmuir and Freundlich isotherms to evaluate the adsorption capacities of both adsorbents.

The Langmuir isotherm assumes that molecules adsorbed on an adsorbent do not react with each other, and it is valid for monolayer adsorption on the surface of the adsorbent including a finite number of identical sites. A basic assumption is that sorption takes place at specific homogeneous sites within the adsorbent. A well known linear form of Langmuir equation can be expressed as [29, 30]:

$$C_e/q_e = 1/(b \times q_m) + C_e/q_m \quad (4)$$

where q_m represents amount of adsorbate required to form a monolayer (mg/g), and q_e is adsorbate uptake at equilibrium (mg/g). C_e is the equilibrium concentration (mg/L), and b is Langmuir constant (L/mg). The values of b and q_m can be calculated from the intercept and slope of the plot C_e/q_e versus C_e. An important feature of the Langmuir isotherm is R_L, which is a dimensionless equilibrium parameter, also known as the separation factor, defined as [31]:

$$R_L = 1/(1 + bC_i) \quad (5)$$

where C_i is the same as defined above.

The value of R_L in the range of 0~1 indicates favorable adsorption, while $R_L > 1$ represents unfavorable adsorption; $R_L = 1$ hints linear adsorption while the adsorption process is irreversible in the event of $R_L = 0$.

The Freundlich isotherm is valid for multilayer adsorption on the surface of an adsorbent, indicating nonideal adsorption on heterogeneous surfaces. The linear form of the Freundlich equation is given as follows [32]:

$$\ln q_e = \ln K_F + 1/n \ln C_e \quad (6)$$

where K_F ((mg/g)(L/mg)$^{1/n}$) and $1/n$ are Freundlich constants, correlated to adsorption capacity and adsorption

Table 3 The pseudo-first-order and pseudo-second-order model parameters for MB onto adsorbents

Samples	Pseudo-first-order model				Pseudo-second-order model		
	q_{exp} mg/g	q_{1e} mg/g	k_1 min^{-1}	R^2	q_{2e} mg/g	$k_2\times10^{-4}$ g/(mg min)	R^2
CTS-*g*-PAA	2,029.98	1,169.20	0.21	0.97229	2,034.58	12.1	1
CTS-*g*-PAA/10% BT	2,016.44	1,357.31	0.18	0.98214	2,023.97	7.04	0.99998

intensity of an adsorbent, respectively. The intercept and slope of the plot of ln q_e against ln C_e can be obtained K_F and $1/n$, respectively.

Correlation coefficients (R^2) and other parameters computed by fitting the experimental equilibrium data to Langmuir and Freundlich isotherm equations were tabulated in Table 4. The best-fit model was determined corresponding to R^2 value. From Table 4, by checking the R^2 values, it indicated that Langmuir model was more suitable for the experimental data due to higher R^2 values, nearly close to unit at all temperatures, suggesting the monolayer coverage of MB on the surfaces of both adsorbents. Furthermore, the experimental adsorption capacities (q_e) were close to theory maximum adsorption capacities (q_m), and the time-rate curves substantially validated the conclusion mentioned above. The values of R_L were in the range of 0~1, indicating that the adsorption process was favorable.

Adsorption thermodynamics

The thermodynamic parameters are important to understand the effect of temperature on the adsorption and to conclude whether the adsorption process is spontaneous or not [33]. In this case, it is necessary to estimate the thermodynamic parameters like Gibbs free energy change (ΔG^0), enthalpy change (ΔH^0), and entropy change (ΔS^0). ΔG^0 related with the equilibrium constant K (L/mol) corresponding to the reciprocal of the Langmuir constant b, can be obtained by the following equation [34]:

$$\Delta G^0 = -\mathrm{R}T\ln b \tag{7}$$

where R is universal gas constant (8.314 J/(mol K)), and T is absolute temperature (K). ΔH^0 and ΔS^0 can be determined by the equation listed below:

$$\ln b = \Delta S^0/\mathrm{R} - \Delta H^0/\mathrm{R}T \tag{8}$$

Correspondingly, ΔH^0 and ΔS^0 can be calculated from the slope and intercept of the plot of ln b against $1/T$, respectively. The results from calculation showed that the overall values of ΔG^0 (−35.27, -37.05, and −35.52 kJ/mol for CTS-*g*-PAA/MB system, −37.46, −36.64, and −37.55 kJ/mol for CTS-*g*-PAA/10% BT/MB system at 30, 40, and 50 °C, respectively) during the adsorption were negative in the range of the temperature studied, indicating that the adsorption process was feasible and spontaneous in nature. It was obvious that the values of ΔH^0 (−14.35 and −16.41 kJ/mol for CTS-*g*-PAA/MB system and CTS-*g*-PAA/10% BT/MB system, respectively) were negative, indicating the adsorption of MB onto both adsorbents was exothermic and the little values of ΔH^0 revealing that physisorption occurred, thereby demonstrating that the adsorption process is stable energetically [35]. The positive values of ΔS^0 (68.96 and 66.46 J/(mol K) for CTS-*g*-PAA/MB system and CTS-*g*-PAA/10% BT/MB system, respectively) corresponding to an increase randomness at the solid/solution interface during the adsorp-

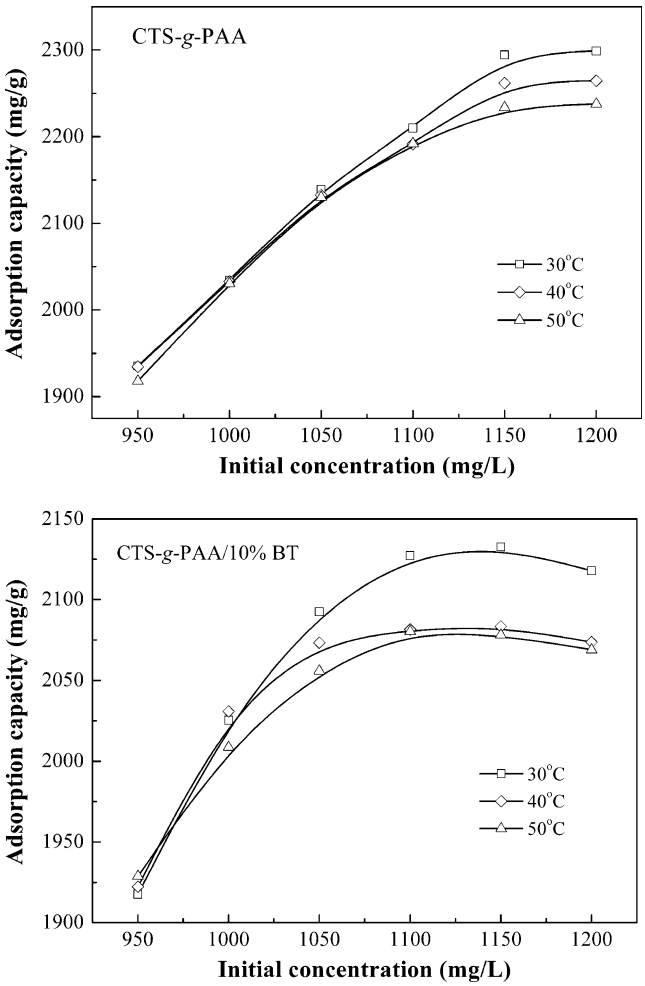

Fig. 4 Effect of initial concentration and temperature on adsorption

Table 4 Isotherm constants for MB on adsorbents

Adsorbent		Langmuir model					Freundlich model		
	t °C	q_e mg/g	q_m mg/g	b L/mg	R^2	$R_L \times 10^4$	K_F (mg/g)(L/mg)$^{1/n}$	$1/n$	R^2
CTS-*g*-PAA	30	2,298.95	2,315.80	3.20	0.99994	2.60~3.29	1,962.08	0.0486	0.66455
	40	2,264.52	2,277.30	2.61	0.99998	3.19~4.03	1,927.71	0.0450	0.72527
	50	2,237.67	2,252.34	2.25	0.99998	3.70~4.67	1,903.81	0.0427	0.73147
CTS-*g*-PAA/10% BT	30	2,132.58	2,125.70	4.74	0.99998	1.76~2.22	1,903.79	0.0255	0.79119
	40	2,083.41	2,080.00	5.51	0.99998	1.51~1.91	1,905.52	0.0194	0.71425
	50	2,080.29	2,076.74	3.14	0.99998	2.65~3.35	1,883.66	0.0209	0.83977

tion of MB onto adsorbents, suggested the affinity of the adsorbents for MB.

Adsorption mechanism

The FTIR spectra of CTS-*g*-PAA and CTS-*g*-PAA/10% BT before and after MB adsorption, and the molecular structure of MB were shown in Fig. 5, to well understand adsorption mechanism. Combined with the molecular structure of MB (Fig. 5 (1)), the bands at 1,609, 1,538, 1,490, and 1,440 cm^{-1} (Fig. 5 (2)), related with stretching vibration of C–C bond of aromatic cycle of MB molecule were shifted, broadened, and reduced after adsorption for both adsorbents. Furthermore, the three absorption bands (1,538, 1,490, and 1,440 cm^{-1}) were overlapped with C=O asymmetric and symmetric stretching vibration after adsorption. The characteristic absorption peaks of aromatic skeletal groups (881, 840, and 803 cm^{-1}) were shifted and broadened after adsorption for both adsorbents. All these findings indicated that MB onto both adsorbents was held by physisorption, like electrostatic attraction or ion exchange.

Desorption studies was also helpful in elucidating the adsorption mechanism of an adsorption process. If a dye loaded onto an adsorbent can be desorbed by distilled water, it indicates that the attachment of the dye onto the adsorbent is by weak bonds. If strong acids, like hydrochloric acid can desorb the dye, it can be said the attachment of the dye onto the adsorbent is by ion exchange or electrostatic attraction [36]. Consequently, distilled water and 0.1 M hydrochloric acid were used in the elution of MB from the MB loaded hydrogels. The results showed that low desorption efficiencies were obtained (2.41 and 4.67% for CTS-*g*-PAA/MB and CTS-*g*-PAA/10% BT/MB systems, respectively) with distilled water as desorption agent, while 0.1 M hydrochloric acid solution could give the highest recovery for MB (approximate 100% for both adsorbents), indicating MB adsorption onto the hydrogels conducted significantly via electrostatic attraction or ion exchange, which further validated the viewpoints of FTIR analysis.

Conclusions

The MB removal by CTS-*g*-PAA/10% BT was systematically studied under various conditions. The adsorption capacities were found to increase as increasing pH, contact time, and initial concentration, but the adsorption was inhibited by increasing BT content and temperature. The dynamic behavior for MB adsorption onto both adsorbents

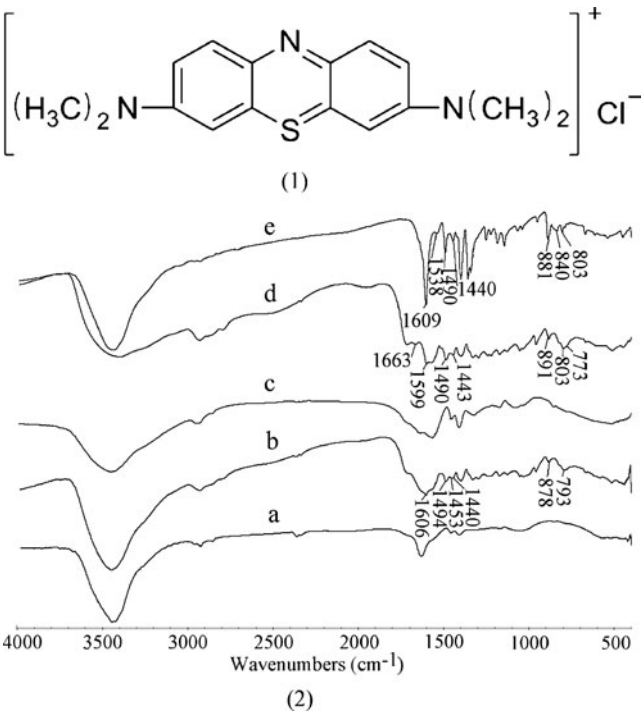

Fig. 5 *1* The molecular structure of MB. *2* The FTIR spectra of CTS-*g*-PAA/10% BT (*a*), MB loaded CTS-*g*-PAA/10% BT (*b*), CTS-*g*-PAA (*c*), MB loaded CTS-*g*-PAA (*d*), and MB (*e*)

preferably obeyed pseudo-second-order kinetics. The Langmuir rather than the Freundlich isotherm model fitted well to describe the adsorption equilibrium data for both adsorbents. The thermodynamic studies indicated that MB adsorption onto both adsorbents was spontaneous and exothermic in nature. The small values of ΔH^0, FTIR spectra analysis, and desorption experiments suggested that electrostatic attraction or ion exchange were responsible for binding of MB with above mentioned adsorbents. By comparison with other hydrogels with the same content of clays, CTS-*g*-PAA/10% BT exhibited much higher adsorption capacity toward MB. CTS-*g*-PAA/10% BT was shown to be a promising adsorbent for MB removal from aqueous solution, and therefore, it could be employed to the related industrial and environmental areas.

Acknowledgments The authors thank for jointly supporting by National Natural Science Foundation of China (No. 20877077) and the Project of Jiangsu Provincial Science and Technology Office (No. BE2008087).

References

1. Raghu S, Basha CA (2007) Chemical or electrochemical techniques, followed by ion exchange, for recycle of textile dye wastewater. J Hazard Mater 149:324
2. Zhu M-X, Lee L, Wang H-H, Wang Z (2007) Removal of an anionic dye by adsorption/precipitation processes using alkaline white mud. J Hazard Mater 149:735
3. Zhang J, Lee K-H, Cui L, Jeong T (2009) Degradation of methylene blue in aqueous solution by ozone-based processes. J Ind Eng Chem 15:185
4. Yan L, Shuai Q, Gong X, Gu Q, Yu H (2009) Synthesis of microporous cationic hydrogel of hydroxypropyl cellulose (HPC) and its application on anionic dye removal. Clean-Soil Air Water 37:392
5. MdT U, Md R, MdMR K, MdA I (2009) Adsorption of methylene blue from aqueous solution by jackfruit (Artocarpus heteropyllus) leaf powder: a fixed-bed column study. J Environ Manage 90:3443
6. Badawy NA, El-Bayaa AA, Alkhalik EA (2010) Vermiculite as an exchanger for copper(II) and Cr(III) ions, kinetic studies. Ionics 16:733
7. Doğan M, Abak H, Alkan M (2009) Adsorption of methylene blue onto hazelnut shell: kinetics, mechanism and activation parameters. J Hazard Mater 164:172
8. El-Said AG, Badawy NA, Abdel-Aal AY, Garamon SE (2010) Optimization parameters for adsorption and desorption of Zn(II) and Se(IV) using rice husk ash: kinetics and equilibrium. Ionics. doi:10.1007/s11581-010-0505-3
9. Crompton KE, Prankerd RJ, Paganin DM, Scott TF, Horne MK, Finkelstein DI, Gross KA, Forsythe JS (2005) Morphology and gelation of thermosensitive chitosan hydrogels. Biophys Chem 117:47
10. Paulino AT, Guilherme MR, Reis AV, Campese GM, Muniz EC, Nozaki J (2006) Removal of methylene blue dye from an aqueous media using superabsorbent hydrogel supported on modified polysaccharide. J Colloid Interface Sci 301:55
11. Bekiari V, Sotiropoulou M, Bokias G, Lianos P (2008) Use of poly(*N*, *N*-dimethylacrylamide-co-sodium acrylate) hydrogel to extract cationic dyes and metals from water. Colloids Surf A 312:214
12. Lin J, Wu J, Yang Z, Pu M (2001) Synthesis and properties of poly(acrylic acid)/mica superabsorbent nanocomposite. Macromol Rapid Commun 22:422
13. Wang L, Zhang J, Wang A (2008) Removal of methylene blue from aqueous solution using chitosan-*g*-poly (acrylic acid)/montmorillonite superadsorbent nanocomposite. Colloids Surf A 322:47
14. Liu Y, Zheng Y, Wang A (2010) Enhaced adsorption of Methylene Blue from aqueous solution by chitosan-*g*-poly (acrylic acid)/vermiculite hydrogel composites. J Environ Sci 22:486
15. Santiago F, Mucientes AE, Osorio M, Poblete FJ (2006) Synthesis and swelling behaviour of poly (sodium acrylate)/sepiolite superabsorbent composites and nanocomposites. Polym Int 55:843
16. Zheng Y, Wang A (2009) Evaluation of ammonium removal using a chitosan-*g*-poly (acrylic acid)/rectorite hydrogel composite. J Hazard Mater 171:671
17. Wang L, Zhang J, Wang A (2011) Fast removal of methylene blue from aqueous solution by adsorption onto chitosan-*g*-poly (acrylic acid)/attapulgite composite. Desalination 266:33
18. Akelah A (1996) Polymer–clay nanocomposites: free-radical grafting of polystyrene on to organophilic montmorillonite interlayers. J Mater Sci 31:3589
19. Lee W-F, Yang L-G (2004) Superabsorbent polymeric materials. XII. effect of montmorillonite on water absorbency for poly (sodium acrylate) and montmorillonite nanocomposite superabsorbents. J Appl Polym Sci 92:3422
20. Li A, Wang A, Chen J (2004) Studies on poly (acrylic acid)/attapulgite superabsorbent composite. I. synthesis and characterization. J Appl Polym Sci 92:1596
21. Wang S, Boyjoo Y, Choueib A (2005) A comparative study of dye removal using fly ash treated by different methods. Chemosphere 60:1401
22. Zohra B, Aicha K, Fatima S, Nourredine B, Zoubir D (2008) Adsorption of Direct Red 2 on bentonite modified by cetyltrimethylammonium bromide. Chem Eng J 136:295
23. Lee JW, Kim SY, Kim SS, Lee YM, Lee KH, Kim SJ (1999) Synthesis and characteristics of interpenetrating polymer network hydrogel composed of chitosan and poly(acrylic acid). J Appl Polym Sci 73:113
24. Senthilkumaar S, Varadarajan PR, Porkodi K, Subbhuraam CV (2005) Adsorption of methylene blue onto jute fiber carbon: kinetics and equilibrium studies. J Colloid Interface Sci 284:78
25. Lagergren S (1898) About the theory of so-called adsorption of soluble substances. Kung Sven Veten Hand 24:1
26. Ho YS, McKay G (1999) Pseudo-second order model for sorption processes. Process Biochem 34:451
27. Srivastava VC, Swamy MM, Mall ID, Prasad B, Mishra IM (2006) Adsorptive removal of phenol by bagasse fly ash and activated carbon: equilibrium, kinetics and thermodynamics. Colloids Surf A 272:89
28. Al-Qodah Z (2000) Adsorption of dyes using shale oil ash. Water Res 34:4295
29. Langmuir I (1918) The adsorption of gases on plane surfaces of glass, mica and platinum. J Am Chem Soc 40:1361
30. Ho YS, Huang CT, Huang HW (2002) Equilibrium sorption isotherm for metal ions on tree fern. Process Biochem 37:1421
31. Hall KR, Eagleton LC, Acrivos A, Vermeulen T (1966) Pore- and solid-diffusion kinetics in fixed-bed adsorption under constant-pattern conditions. Ind Eng Chem Fundam 5:212

32. Freundlich HMF (1906) Über die adsorption in lösungen. Z Phys Chem 57A:385
33. Seki Y, Yurdakoç K (2006) Adsorption of promethazine hydrochloride with KSF montmorillonite. Adsorption 12:89
34. Silva JP, Sousa S, Rodrigues J, Antunes H, Porter JJ, Gonçalves I, Dias SF (2004) Adsorption of acid orange 7 dye in aqueous solutions by spent brewery grains. Sep Purif Technol 40:309
35. Yu Y, Zhuang Y-Y, Wang Z-H (2001) Adsorption of water-soluble dye onto functionalized resin. J Colloid Interface Sci 242:288
36. Mall ID, Srivastava VC, Kumar GVA, Mishra IM (2006) Characterization and utilization of mesoporous fertilizer plant waste carbon for adsorptive removal of dyes from aqueous solution. Colloids Surf A 278:175